Hard radio spectra from reconnection regions in galactic nuclei

G.T. Birk[1], A. R. Crusius–Wätzel[1] and H. Lesch[1]

Institut für Astronomie und Astrophysik der Universität München, D-81679 München, Germany

ABSTRACT

Extremely flat and inverted radio spectra as observed in galactic nuclei and BL Lac sources are still a challenge for fast particle acceleration models. Continuous acceleration by electric fields in reconnection regions can result in almost constant particle distributions and thereby in inverted synchrotron spectra independent from the details of the injected spectrum. These spectra are calculated from a spatially averaged diffusion transport equation in momentum space that includes systematic momentum gains and losses as well as finite particle escape lifetimes.

Subject headings: Galaxies: nuclei – BL Lacaertae objects: general – Radio continuum: galaxies – Acceleration of particles

1. Introduction

Flat and even inverted radio spectra, $I_\nu \sim \nu^{-\alpha}$ with $\alpha < 0$, are a common feature of the non-thermal emission of galactic nuclei. For example Sgr A*, the very center of the Milky Way, as well as the galactic center arc region (Lesch and Reich 1992; Duschl and Lesch 1994) exhibit an inverted spectrum with $\alpha \geq -1/3$. The same holds for the nucleus of M81 (Reuter and Lesch 1996). Slee et al. (1994) found that compact radio continuum cores in about 70 % of radio emitting elliptical and S0 galaxies have a flat or inverted spectrum with a median spectral index of $\alpha = -0.3$. Observations of the Seyfert galaxy NGC 1068 indicate an inverted spectrum with index $\alpha = -0.3$, as well (Muxlow et al. 1996). For active galactic nuclei (AGN) radio surveys by Kühr et al. (1981) and Rayner et al. (2000) have accumulated a huge wealth of data about flat radio spectra. Of special interests are the flat radio spectra of the BL Lac sources Mrk 421 (Tosti et al. 1998) and Mrk 501 (Edwards et al. 2000), both also strong TeV-emitters. However, AGNs and BL Lacs exhibit relatively steep power-law spectra at frequencies higher than the radio regime. The complete electromagnetic spectrum

[1]also: Centre for Interdisciplinary Plasma Science (CIPS), Garching, Germany

of these objects is a result of different energy loss and gain mechanisms. Consequently, the total spectra show flat and steep power-law spectra up to the radiation cut-off (Miller et al. 1996; Terzian et al. 1999). Flat spectrum radio sources are known to be variable over the entire accessible part of the electromagnetic spectrum down to the shortest timescales probed so far (Wagner 1998).

Flat spectrum radio spectra have been attributed to self absorption. For the self-absorption peak frequency to extend over some decades specific geometrical properties in the source are required - this is well known as "cosmic conspiracy" (Marscher 1977; Cotton et al. 1980). This model depends on the source size as $I_\nu \propto \nu r$, where r is the radius of a conical geometry. It implies that the linear size of the source is inversely proportional to the emission frequency, which is not supported by interferometric data (Cotton et al. 1980). Of special interest is the galactic center region, in which it was clearly proven that its flat radio spectrum is not due to self absorption (Lesch et al. 1988; Yusef-Zadeh 1989).

The evidence for flat, optically thin radio spectra in several active galactic nuclei has been presented by Hughes et al. (1989); Melrose (1996); Wang et al. (1997). All these authors consider different Fermi-like acceleration schemes (either multiple shocks or second order Fermi mechanism) to be responsible for the hardness of the electron energy spectra.

In the present contribution it is suggested that optically thin synchrotron emission due to hard electron spectra produced in magnetic reconnection regions can explain the nature of the flat/inverted spectrum radio sources.

2. Particle acceleration in reconnection regions

Any acceleration model of charged particles must ultimately be based on the energy gain of the particles in electric fields. However, the dynamics of the respective plasma processes involved can be quite different. The principal acceleration scenarios (reviews are given, e.g., by Schlickeiser (1986); Kirk (1994); Kuijpers (1996)) may be divided in the Fermi I and Fermi II mechanisms, shock-drift acceleration (which in fact can be considered as an example of Fermi I acceleration), diffusive shock acceleration, plasma wave acceleration, electrostatic double layers and the energization of particles in reconnection events. In contrast to the other 'classic' mechanisms it was only more recently that reconnection was discussed as a process that does not only convert magnetic field energy to plasma bulk motion and heating but also plays an important role in the context of fast particle acceleration (Schindler et al. 1991; Vekstein and Priest 1995; Lesch and Birk 1998; Schopper et al. 1998; Litvinenko 1997, 1999).

In the context of shock acceleration much elaborated work has been done concerning the shape and evolution of the energy distribution of the accelerated particles (e.g. Kuijpers (1996); Achterberg (2000) and ref. therein). One may note that in the diffusive shock scenarios the injection problem appears, i.e. one has to assume a high-energy electrons to start with. Within many applications only the modification of power law spectra by shocks which are assumed for the injected particle population in the first place are investigated. What is more, very flat spectra are very hard to explain in the context of simple shock acceleration (Melrose 1996).

Nothing comparable to the detailed studies on the energy spectra of shock accelerated particles has been done for the reconnection scenario. In this contribution we analyze the energy spectra that can be expected to be caused by high-energy particles accelerated in dc electric fields in reconnection regions starting from the space-averaged transport equation for the one-particle distribution function that represents the high-energy particle component.

In three-dimensional configurations with $B \neq 0$ everywhere a finite electric field component parallel to the magnetic field E_s is necessary for the onset of magnetic reconnection (Hesse and Schindler 1988; Schindler et al. 1991). Ideal Ohm's law is to be violated

$$\mathbf{E} + \frac{1}{c}\mathbf{v} \times \mathbf{B} = \mathbf{R} \neq 0 \tag{1}$$

where $\mathbf{R}$ is some yet unspecified non-idealness. In the associated generalized electric potential (Schindler et al. 1988, 1991)

$$U = -\int E_s ds = -\int R_s ds, \tag{2}$$

where the integral is evaluated along the magnetic field lines that penetrate the reconnection region, charged particles can be efficiently accelerated. It should be mentioned that in general U is not an electrostatic potential. Note that particles are not necessarily accelerated up to energies associated with U but expression (2) gives an upper limit of the energy level of the accelerated particle population. The electric potentials are often associated with non-ideal flows like steady rotational motion or (non-)stationary shear flows. The nature of the non-idealness $\mathbf{R}$ and the reconnection process determines the strength, structure and time dependence of the electric potential and thereby the particle energization. One can think of different kinds of non-idealness in Ohm's law that allow for the reconnection process to start. Since astrophysical plasmas are on large spatial scales highly collisionless the Coulomb resistivity is negligible. Nevertheless, Ohm's law can locally be violated by $R_s = \eta j_s$, where j_s is the magnetic field aligned component of the current density, provided that some anomalous resistivity η is caused by microturbulent stochastic electromagnetic fields (e.g. Huba (1985) and ref. therein). The microturbulence can be caused by currents.

When the current density exceeds a critical value, unstable kinetic waves can be excited that in their non-linear evolution result in stochastic microturbulent electromagnetic fields. The same concept $R_s \sim j_s$ for $j > j_{crit}$ holds for stochastic ion acoustic double layers as a source for anomalous dissipation (Haerendel 1993). In relativistic plasmas, in particular, finite particle inertia can be responsible for the non-idealness $R_s \sim \partial j_s/\partial t + \nabla \cdot (\mathbf{vj} + \mathbf{jv})$ as was recently discussed in the context of extragalactic jets (Lesch and Birk 1998).

In the present study we are rather interested in the resulting power-law indices of the energy spectra of the high-energy particles than in their maximum energy. The spectra result from the combined effects of direct acceleration of charged particles in the dc electric fields in reconnection regions and radiative loss processes. For the acceleration the yet unspecified quantity R_s plays the crucial role. In the simplest standard scenario of two-dimensional stationary reconnection a constant electric field perpendicular to the plane where a projection of one magnetic field component changes sign occurs, e.g., (Parker 1963; Biskamp 1993). This electric field is a result of the non-idealness R_s that is assumed to be constant in the reconnection region. Let us now consider a configuration with a dominant constant magnetic field component parallel to the direction of the associated electric current. The electric field parallel to this magnetic field component is approximately E_s and therefore the fast particle acceleration is constant in time. A finite pitch angle of the accelerated particles allows for the radiative losses. To be more specific let us consider a generic shear configuration. If a plasma flow, say $\mathbf{v}_s = v_s(x,z)\mathbf{e}_y$ is applied to an homogeneous magnetic field $\mathbf{B} = B_z\mathbf{e}_z$ a shear component forms $B_y = \int B_z \partial v_s/\partial z dt$ that results, in particular, in an electric current flowing parallel to B_z. Given some localized dissipation (caused, e.g., by a supercritical current density) magnetic reconnection can take place. In a stationary state a constant (Biskamp 1993) inflow $\mathbf{v}_i = v_i\mathbf{e}_x$ towards the reconnection region occurs and the magnetic shear is converted to heat and kinetic energy as fast as it is built up by the external shear flow v_s. The convergent velocity v_i can be expressed as a function of the local Alfvén velocity and the (constant) reconnection rate (Biskamp 1993). The quasi-stationary magnitude of the electric field component that causes the acceleration of fast particles along B_z can then be estimated without specifying for the non-idealness R_s as it is possible in a more elaborated general three-dimensional reconnection model (Schindler et al. 1988, 1991). In our example, we find

$$E_z \approx \frac{1}{\Delta_{\rm rec} c} \int_{\Delta_{\rm rec}} dz \int_T dt v_i \frac{\partial B_y}{\partial t} \tag{3}$$

where $\Delta_{\rm rec}$ and T denote the extent of the reconnection region along B_z and the typical time scale of shear formation.

In what follows, we describe the particle acceleration by a an average constant electric field. In particular, the acceleration force does not depend on the momentum of the charged

particles.

3. The momentum balance equation for the accelerated particle population

The population of high-energy particles that do not interact with each other can be described by the one-body distribution function $f(\mathbf{r}, \mathbf{p}, t)$ that obeys the Liouville equation

$$\frac{\partial f}{\partial t} + \frac{d\mathbf{r}}{dt}\nabla_{\mathbf{r}} f + \frac{d\mathbf{p}}{dt}\nabla_{\mathbf{p}} f = 0. \tag{4}$$

Though this equation contains the full dynamical information it is of limited use since this non-linear differential equation in seven variables is usually unsolvable for physical situations of interest. Fortunately, we need not to know the full information of the particle dynamics in a rigorous manner. First, will assume pitch angle isotropy. This idealization is motivated by the fact that in reconnection regions Alfvénic and magnetosonic wave fields with relatively high-energy densities are to be expected which cause an efficient particle scattering in momentum space (Schlickeiser 1986). Additionally, self-excited Alfvén turbulence maintain quasi-isotropy, if the systematic velocity of the high-energy particles exceeds the Alfvén speed of the ambient plasma (Kuijpers 1996). Second, when asking about the energy spectrum of the accelerated particles in a specified astrophysical object the detailed spatial dependence of the distribution function is often of no interest. Rather it is usually sufficient to concentrate on a distribution function space-averaged over the volume V. Thus, we deal with the isotropic distribution $f'(p,t) = \int d\mathbf{r} f(\mathbf{r}, p, t)/V$. The total particle number is calculated as $N(t) = 4\pi \int f' p^2 dp$. The loss in information is not too high a price to pay in order to obtain a transport equation in momentum space one can really deal with. The continuous momentum gains and losses Δp the particles experience can be described by a momentum operator

$$\mathcal{L}_p = \frac{1}{p^2}\frac{\partial}{\partial p}[(\dot{p}_{gain} + \dot{p}_{loss})p^2], \tag{5}$$

if one concentrates, as in the present study, on systematic temporal momentum gains $\dot{p}_{gain}$ and losses $\dot{p}_{loss}$. The finite characteristic time τ a particle stays in the acceleration region gives rise to a further sink in the balance equation for $f'(p,t)$. In the reconnection scenario particles can escape $E_s \neq 0$-regions by following reconnected field-lines outward the non-ideal regions. Some explicit source term $S(p)$, on the other hand, represents the injected particle population. Taking these effects into account the temporal evolution of the particle distribution is governed by the equation (Jones 1970; Schlickeiser 1984, 1986)

$$\frac{\partial f'(p,t)}{\partial t} + \mathcal{L}_p f'(p,t) + \frac{f'(p,t)}{\tau} = S(p) \tag{6}$$

which holds, if the distribution function $f(\mathbf{r}, p, t)$ is separable in the space and the momentum variables, and if the momentum operator $\mathcal{L}_p$ is space independent.

It should be noted that equations(5) and (6) hold only for momentum changes $\Delta p \ll p$ during a time interval $\Delta t \ll \tau$. If one wants to include the effects of stochastic diffusion in momentum space, which may become important, e.g., for a microturbulent resistivity, a Fokker-Planck diffusion term could be incorporated (Schlickeiser 1984, 1986) in equation(5).

The momentum change terms in equation(5) in our case can be specified as follows. The dominant loss processes that are mainly responsible for the non-thermal radiative phenomena are synchrotron and inverse Compton radiation. We will not consider Bremsstrahlung ($\dot{p}_{loss} \sim p$) here, since this effect usually is dominated by the other ones mentioned. Both processes scale as (Longair 1981) $\dot{p}_{loss} = -kp^2$ with $k = \frac{4}{3}\sigma_{\mathrm{T}} c^2 U$ where σ_{T} is the Thomson cross-section and U is the magnetic field or photon energy density, respectively. The momentum gain of a single charged particle in the acceleration region is given by

$$\dot{p}_{gain} = \frac{d}{dt}(\gamma m v) = qE_s = qR_s \tag{7}$$

where γ is the Lorentz factor and q is the electrical charge. In this contribution we exclusively consider the case $qR_s = \zeta$ =const. (see discussion in section 2) and thus, solve the transport equation

$$\frac{\partial f}{\partial t} + \left(\frac{2\zeta}{p} - 4kp\right) f + \left(\zeta - kp^2\right) \frac{\partial f}{\partial p} + \frac{f}{\tau} = S(p) \tag{8}$$

where the primes are now omitted. Equations of this kind can, in general, be solved by means of the inverse Laplace transformation (Melrose 1980).

4. Power law particle distributions

First, we solve the steady-state version of equation(8) for different source populations. The resulting distribution function reads

$$f(p) = f_0 p^{-2} |\zeta - kp^2|^{-1} \left| \frac{1 + p\sqrt{k/\zeta}}{1 - p\sqrt{k/\zeta}} \right|^{-\frac{1}{2\tau\sqrt{k\zeta}}} \tag{9}$$

where f_0 depends on the injected source population by the integral

$$f_0 = \int^p p'^2 \left| \frac{1 + p'\sqrt{k/\zeta}}{1 - p'\sqrt{k/\zeta}} \right|^{\frac{1}{2\tau\sqrt{k\zeta}}} S\left(p'\right) dp'. \tag{10}$$

If the acceleration is negligible as compared to radiative losses, the stationary energy spectrum equation(9) shows the pure aging behavior (see Longair (1981)) caused by synchrotron or inverse Compton losses $f(p) \sim p^{-4}$ where $f(p)dp$ is the particle number in the momentum interval dp. If the losses are negligible, the spectrum is given by $f(p) \sim p^{-2}e^{-p/\zeta\tau}$.

We note that the distribution function given by equation(9) may diverge at the momentum $p = p_c = \sqrt{\zeta/k}$ where gains and losses balance. When it is rewritten as

$$f(p) = f_0 k \left(\frac{p}{p_c}\right)^{-2} \left(1 + \frac{p}{p_c}\right)^{-\frac{1}{2\tau\sqrt{k\zeta}}-1} \left|1 - \frac{p}{p_c}\right|^{\frac{1}{2\tau\sqrt{k\zeta}}-1} \tag{11}$$

it becomes clear that the function is well behaved for $2\tau\sqrt{k\zeta} < 1$, with $f(p_c) = 0$. A pile-up of particles occurs if $2\tau\sqrt{k\zeta} > 1$. This is equivalent to $\tau > \sqrt{t_{acc}t_{loss}}/2$ if one defines the acceleration and loss timescale as $\dot{p}_{gain} = p/t_{acc} = \zeta$ and $\dot{p}_{loss} = -p/t_{loss} = -kp^2$, respectively. This means that the particles are collected near $p = p_c$ when the escape time (which depends on the geometry of the acceleration region) is longer than half the geometric mean of the timescales for acceleration and radiative losses. Otherwise the particles escape before they can accumulate.

It needs mentioning that the pile-up at the critical momentum $p_c = \sqrt{\zeta/k}$ would be smoothed out, if a Fokker-Planck diffusion term was incorporated in equation(8). This was done by Schlickeiser (1984) for the case of shock acceleration.

We now turn to determine f_0 in equation(9) for different injection spectra. For a monoenergetic source population $S(p) = s_0\delta(p - p_0)$ we find

$$f_0 = s_0 p_0^2 \Theta(p - p_0) \left(\frac{1 + p_0\sqrt{k/\zeta}}{1 - p_0\sqrt{k/\zeta}}\right)^{\frac{1}{2\tau\sqrt{k\zeta}}} \tag{12}$$

where Θ denotes the Heaviside function. In the next section we will calculate spectra for this source population. For a relativistic Maxwellian source population $S(p) = s_0\exp(-ap)$, where a is a constant, one obtains

$$f_0 = s_0 \int^p p'^2 e^{-ap'} \left|\frac{1 + p'\sqrt{k/\zeta}}{1 - p'\sqrt{k/\zeta}}\right|^{\frac{1}{2\tau\sqrt{k\zeta}}} dp' \tag{13}$$

where c is some integration constant. In the limit of negligible particle escape, i.e. $\tau\sqrt{k\zeta} \to \infty$, or for negligible acceleration as compared to radiative losses $k/\zeta \to \infty$ the particle distribution reads

$$f(p) = \frac{1}{a^3} e^{-ap}(2 + 2ap + a^2p^2)|\zeta - kp^2|^{-1}p^{-2}. \tag{14}$$

For a power law source distribution, $S(p) = s_0 p^{-z}$ f_0, can be determined as

$$f_0 = s_0 \int^p p'^{2-z} e^{-ap'} \left| \frac{1 + p'\sqrt{k/\zeta}}{1 - p'\sqrt{k/\zeta}} \right|^{\frac{1}{2\tau\sqrt{k\zeta}}} dp'. \tag{15}$$

If one considers again the limits of negligible particle escape or negligible acceleration one finds

$$f(p) = s_0 \frac{p^{3-z}}{3-z} |\zeta - kp^2|^{-1} p^{-2}. \tag{16}$$

Non-stationary solutions of equation(8) with an exponential time evolution $f(p,t) \sim e^{-t/\tau}$ can be found provided the distribution function satisfies $\mathcal{L}_p f = S(p)$. For a monoenergetic source population one obtains for $p > p_0$

$$f(p,t) = cp^{-2} |\zeta - kp^2|^{-1} e^{-\frac{t}{\tau}} \tag{17}$$

where the constant c contains s_0. A relativistic Maxwellian source population and a power-law one result in

$$f(p,t) = \left(c + \frac{s_0}{a} e^{-ap} \right) p^{-2} |\zeta - kp^2|^{-1} e^{-\frac{t}{\tau}} \tag{18}$$

and

$$f(p,t) = \left(c + s_0 p^{-z} \right) p^{-2} |\zeta - kp^2|^{-1} e^{-\frac{t}{\tau}}, \tag{19}$$

respectively.

5. Synchrotron emission spectrum

The spectral power P_ν radiated by a single particle with momentum p is in a good approximation given by ($b = \sqrt{3} e^3 B \sin\theta / mc^2$ and $\nu_c = 3eB \sin\theta \, p^2 / 4\pi (mc)^3$, with θ being the angle between the magnetic field and the line of sight)

$$P_\nu(p) = b \left(\frac{\nu}{\nu_c} \right)^{1/3} e^{-\nu/\nu_c}, \tag{20}$$

see Melrose (1980b). It has its maximum near $\nu = \nu_c$ and shows a characteristic $\nu^{1/3}$ spectrum for $\nu \ll \nu_c$ and an exponential cutoff for $\nu \gg \nu_c$. The specific intensity from an isotropic momentum distribution of particle density $N(p) = 4\pi p^2 f(p)$ can then be calculated by

$$I_\nu = \int dp \; N(p) P_\nu(p). \tag{21}$$

In figure (1) we plot the distribution function $N(p) = 4\pi p^2 f(p)$ with $f(p)$ from equation(11) for a monoenergetic source population (equation(12)) with different values of $a = 1/2\tau\sqrt{k\zeta}$. The pile-up results for $a = 0.5$. The higher cut-off results for $a = 2$ and the third curve represents the case $a = 6$. Figure (2) shows the corresponding synchrotron radiation spectra along with the spectrum of a single particle (upper curve) according to equation(20) for comparison. Going downward, the other curves again represent $a = 0.5$, $a = 2$, and $a = 6$, respectively. It is interesting that the low-frequency part becomes flattened even though the particle distribution remains constant at low energies and changes only near the cutoff momentum. The spectral index α with $I_\nu \propto \nu^{-\alpha}$ is given by $\alpha = -0.33$ for the upper curve and $\alpha \approx -0.1$ for the lowest curve. This shows that synchrotron emission with inverted spectra is to be expected from reconnection zones. We note again that in the context of AGNs and BL Lacs the complete emission spectra show power-laws for higher than radio frequencies.

6. Discussion

Particle acceleration by field-aligned electric fields in reconnection regions can be described by diffusion in momentum space as long as the differential momentum changes are small compared to the respective instant particle momentum. This assumption seems not to be that restrictive, since reconnection events are expected to excite intense Alfvénic modes and MHD turbulence that causes efficiently pitch angle diffusion. Thus, in many applications the diffusion treatment seems to be appropriate. The present analysis shows that mainly constant distributions for accelerated particles are to be expected no matter whether monoenergetic, Maxwellian or power law populations are injected into the reconnection regions. The associate synchrotron spectra $I_\nu \propto \nu^{-\alpha}$ show negative spectral indices $\alpha < 0$. Such rising spectra are ubiquitously observed in galactic nuclei (Rayner et al. 2000) as in the core regions of blazars (Edwards et al. 2000).

We stress that the actual acceleration problem is highly involved. Our findings come from a quite simple nonetheless physically reasonable scenario. Highly anisotropic particle distributions cannot be described within our approach. Neither local variations of the spectra can be determined. Whereas some improvement may be possible on the analytical side we feel that a numerical test particle approach and self-consistent electromagnetic particle simulations are indispensable for a deeper understanding of the acceleration of high-energy particles in reconnection regions.

This work has been supported by the Deutsche Forschungsgemeinschaft through the

grant LE 1039/6.

REFERENCES

Achterberg, A. 2000, in Highly Energetic Physical Processes and Mechanisms for Emission from Astrophysical Plasmas, eds. Martens, P.C.H., Tsuruta, S., and Weber, M.A., IAU Symp. 195, San Francisco, p. 291

Biskamp, D. 1993, Nonlinear Magnetohydrodynamics, Cambridge University Press, p.127ff

Cotton, W.D., Wittels, J. J., Shapiro, I. I. et al. 1980, ApJ, 238, L123

Duschl, W., and Lesch, H. 1994, A&A, 286, 431

Edwards, P.G., Giovannini, Cotton, W.D., Feretti, L., Fujisawa, K., Hirabayashi, H., Lara, L., and Venturi, T. 2000, PASJ, 52, 1015

Haerendel, G. 1993, ApJS, 90, 765

Hesse, M., and Schindler, K. 1988, J. Geophys. Res., 93, 5559

Huba, J.D. 1985, in Unstable Current Systems and Plasma Instabilities in Astrophysics, eds. M.R. Kundu and G.D. Holman, IAU Symp. 107, Reidel, Dordrecht, 315

Hughes, P.A., Aller, H.D., and Aller, M.F. 1989, ApJ, 341, 68

Jones, F.C. 1970, Phys. Rev. D, 2, 2787

Kirk, J.G. 1994, in Plasma Astrophysics, eds. A.O. Benz and T.J.-L. Courvoisier, Springer, Berlin, 225

Kuehr, H., Pauliny-Toth, I. I. K., Witzel, A., and Schmidt, J. 1981, AJ, 86, 854

Kuijpers, J. 1996, in Plasma Astrophysics, LNP 468, eds. C. Chiuderi and G. Einaudi, Springer, Heidelberg, 101

Lesch, H., Schlickeiser, R., and Crusius, A. 1988, A&A, 200, L9

Lesch, H., and Reich, W. 1992, A&A, 264, 493

Lesch, H., and Birk, G.T. 1998, ApJ, 499, 167

Litvinenko, Y.E. 1997, Phys. Plasmas, 4, 3439

Litvinenko, Y.E. 1999, A&A, 349, 685

Longair, M.S. 1981, High energy astrophysics, Cambridge University Press

Marscher, A.P. 1977, ApJ, 216, 244

Melrose, D.B. 1980a, Plasma Astrophysics Vol. 2, Gordon & Breach, New York, chap. 9.3

Melrose, D.B. 1980b, Plasma Astrophysics Vol. 1, Gordon & Breach, New York, p. 120

Melrose, D.B. 1996, in Extragalactic Radio Sources, IAU Symp. 175, eds. R. Ekers, C. Fanti, and L. Padrielli, Reidel, Dordrecht, 423

Miller, H.R., Webb, J., Noble, J.C. 1996, Blazar Continuum Variability, ASP Conf. Ser. 110, BookCrafters.

Muxlow, T.W.B., Pedlar, A., Holloway, A.J., Gallimore, J. F., and Antonucci, R. R. J. 1996, MNRAS, 278, 854

Parker, E. N. 1963, ApJS, 8, 177

Rayner, D.P., Norris, R.P., and Sault, R.J. 2000, MNRAS, 319, 484

Reuter, H.P., and Lesch, H. 1996, A&A, 310, L5

Schindler, K., Hesse, M., and Birn, J. 1988, J. Geophys. Res., 93, 5547

Schindler, K., Hesse, M., and Birn, J. 1991, ApJ, 380, 293

Schlickeiser, R. 1984, A&A, 136, 227

Schlickeiser, R. 1986, in Cosmic Radiation in Contemporary Astrophysics, ed. by M.M. Shapiro, Reidel, Dordrecht, 27

Schopper, R., Lesch, H., and Birk, G.T. 1998, A&A, 335, 26

Slee, O.B, Sadler, E.M., Reynolds, J.E., and Ekers, R.D. 1994, MNRAS, 269, 928

Terzian, Y., Weedman, D., Khachikian, E. (eds.) 1999, Active Galactic Nuclei and Related Phenomena, IAU Symp. 194, Astronomical Society of the Pacific.

Tosti, G., Fiorucci, M., Luciani, M., Efimov, Yu. S., Shakhovskoy, N. M., Valtaoja, E., Teraesranta, H., Sillanpaeae, A., Takalo, L. O., Villata, M., Raiteri, C. M., de Francesco, G., and Sobrito, G. 1998, A&A, 339, 41

Vekstein, G.E., and Priest, E.R. 1995, Phys. Plasmas, 2, 3169

Wagner, S.J. 1998, in Radio Emission from Galactic and Extragalactic Compact Sources, IAU Colloq. 164, eds. J.A. Zensus, G.B. Taylor, and J.M. Wrobel, ASP Conf. Series 144, p. 257

Wang, J., Cen, X., Xu, J., and Qian, T. 1997, ApJ, 491, 501

Yusef-Zadeh, F. 1989, in The center of the Galaxy, IAU Symp. 136, ed. M. Morris, Reidel, Dordrecht, 243

Fig. 1.— The particle spectrum in a double-logarithmic representation for $a = 1/2\tau\sqrt{k\zeta}$ (see equation(11) chosen as $a = 0.5$ (pile-up), $a = 2$ (higher cut-off), and $a = 6$ (lower cut-off), respectively.

Fig. 2.— The synchrotron emission spectrum in a double-logarithmic representation. The uppermost curve represents the single-particle spectrum and the following ones represent the cases $a = 0.5$, $a = 2$, and $a = 6$, respectively. The logarithm of the intensity is normalized to its value at $\log(\nu/\nu_c) = -6$.

This preprint was prepared with the AAS LaTeX macros v5.0.

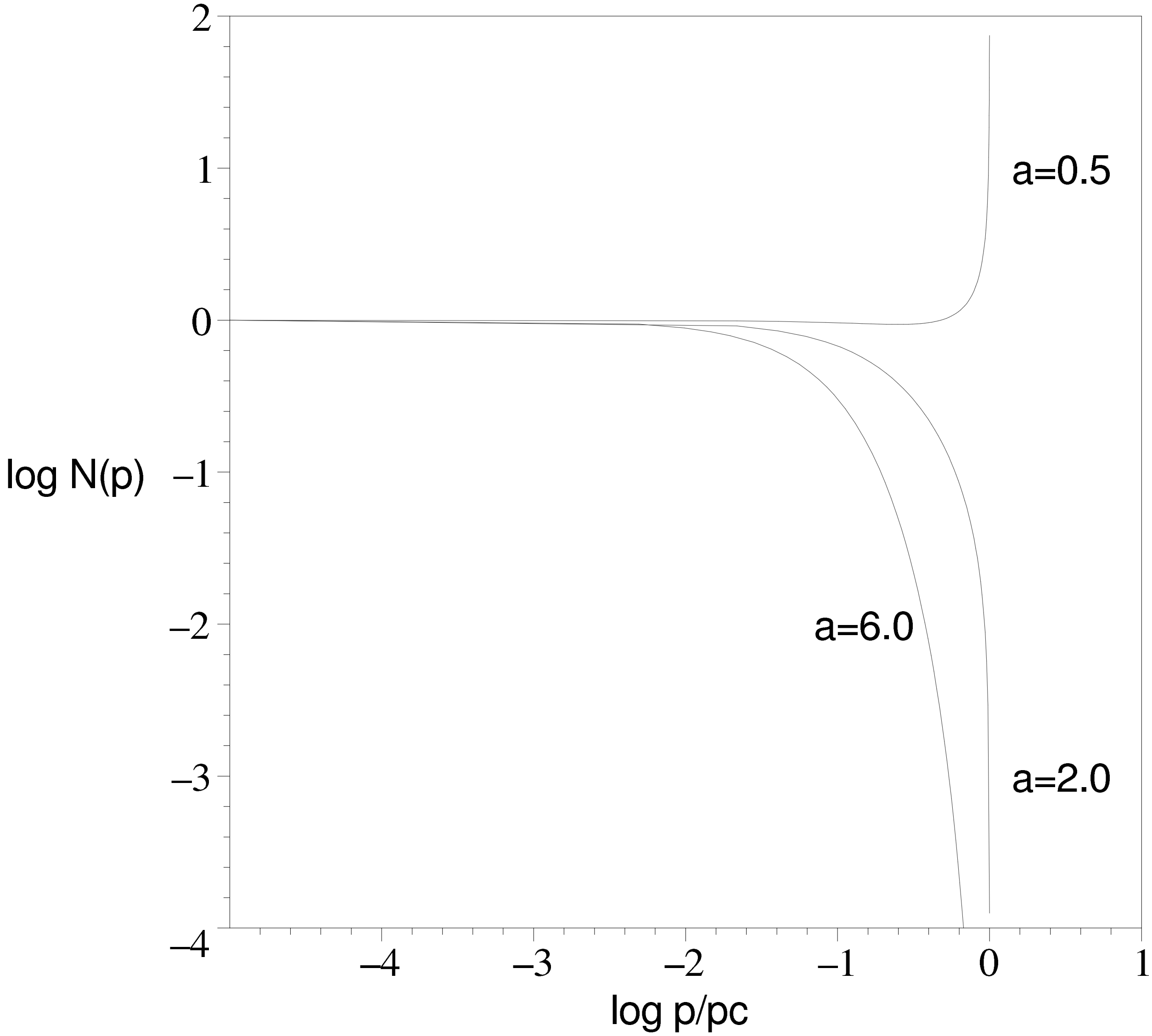
a=0.5
a=6.0
a=2.0
log N(p)
log p/pc
2
1
0
–1
–2
–3
–4
–4
–3
–2
–1
0
1

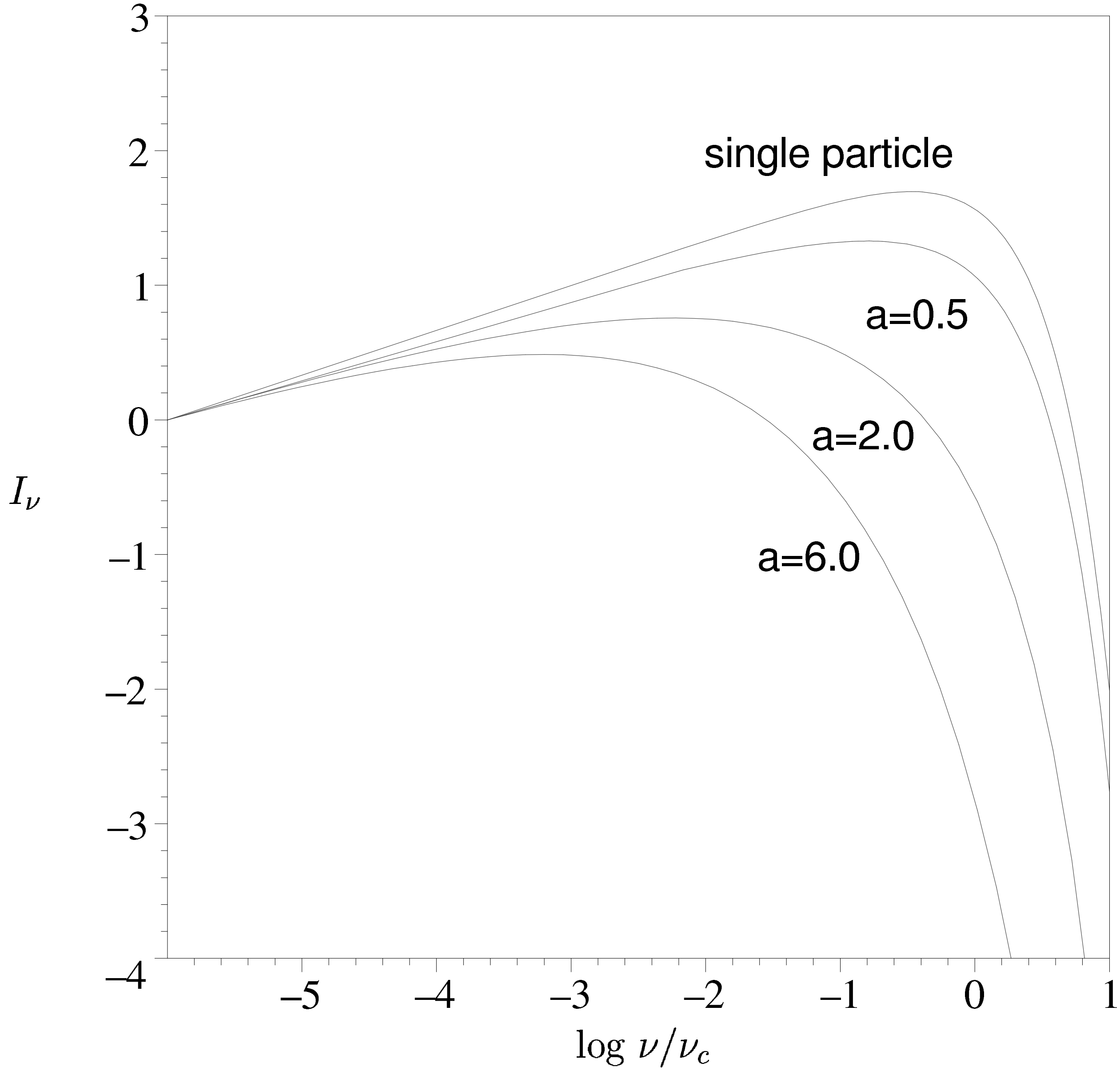
single particle
a=0.5
a=2.0
a=6.0
I_ν
$\log \nu/\nu_c$
3
2
1
0
–1
–2
–3
–4
–5
–4
–3
–2
–1
0
1